Rho activity critically and selectively regulates endothelial cell organization during angiogenesis

Mien V. Hoang, Mary C. Whelan, and Donald R. Senger*

Division of Cancer Biology and Angiogenesis, Department of Pathology, Beth Israel Deaconess Medical Center, and Harvard Medical School, Boston, MA 02215

Communicated by Richard O. Hynes, Center for Cancer Research, Cambridge, MA, December 19, 2003 (received for review August 16, 2002)

The mechanisms that control organization of endothelial cells (ECs) into new blood vessels are poorly understood. We hypothesized that the GTPase Rho, which regulates cytoskeletal architecture, is important for EC organization during neovascularization. To test this hypothesis, we designed a highly versatile mouse skin model that used vascular endothelial growth factor-expressing cells together with packaging cells producing retroviruses encoding RhoA GTPase mutants. In this animal model, dominant negative N19RhoA selectively impaired assembly of ECs into new blood vessels; and, in contrast, active V14RhoA stimulated ECs to form blood vessels with functional lumens. *In vitro*, dominant negative N19RhoA reduced EC actin stress fibers and prevented ECs from contracting and reorganizing into precapillary cords within collagen gels. In contrast, active V14RhoA promoted EC stress fiber formation, contractility, and organization into cords. Neither N19RhoA nor V14RhoA significantly affected EC proliferation or migration *in vitro*; and, similarly, neither mutant significantly affected EC density during angiogenesis *in vivo*. Thus, these studies identify a critical and selective role for Rho activity in regulating EC assembly into new blood vessels, and they identify both negative and positive manipulation of Rho activity, respectively, as strategies for suppressing or promoting the organizational stages of neovascularization.

Angiogenesis, also known as neovascularization, is the formation of new blood vessels through endothelial cell (EC) proliferation and stem cell recruitment in combination with morphogenesis (1, 2). Therapies designed to control angiogenesis, both positively and negatively, offer promise for the treatment of several important pathologies. For example, suppression of angiogenesis is desirable for preventing the blindness associated with proliferative retinopathies (3) and for restricting tumor growth (4). Conversely, for ulcerative pathologies involving vascular insufficiency or for ischemic cardiovascular disease, therapies designed to stimulate angiogenesis offer promise for ulcer healing and restoration of normal tissue function (5).

Vascular endothelial growth factor (VEGF) is a potent hypoxia-inducible cytokine that drives the angiogenesis associated with normal embryonic development, proliferative retinopathies, and cancers (6–8). Consequently, much attention has focused on manipulation of VEGF, either negatively or positively, depending on whether the desired outcome is inhibition or stimulation of angiogenesis (3, 5, 7).

Although the importance of VEGF for angiogenesis is well established, the mechanisms that regulate the morphogenetic process through which proliferating ECs organize into new blood vessels are poorly understood. It is likely that mechanisms that regulate EC morphogenesis act through cytoskeletal elements, and therefore that cytoskeletal regulatory molecules are probably involved. In particular, the GTPase Rho mediates cell contractility by organizing actin filaments into stress fibers (9, 10); and active Rho is required for a variety of complex morphogenetic processes, including embryonic gastrulation (11, 12) and epidermal wound healing (13). Thus, the importance of Rho for these processes is consistent with a possible role in vascular morphogenesis. To test this possibility directly, we used retroviruses encoding established dominant negative and constitutively active RhoA GTPase mutants and designed experiments both *in vivo* and *in vitro* to define Rho function in VEGF-driven angiogenesis. As described here, these RhoA mutants identify a critical and selective function for Rho activity in regulating the assembly of ECs into new blood vessels, and they illustrate the utility of modulating Rho activity, both negatively and positively, as a means either to suppress or promote neovascularization.

Materials and Methods

VEGF, ECs, and Cell Culture. Purified recombinant human $VEGF_{165}$, expressed in Sf21 cells, was obtained from the National Cancer Institute Preclinical Repository, Biological Resources Branch (Frederick, MD). Human dermal microvascular ECs were isolated from neonatal foreskins (14) and cultured as described (15). All experiments were performed with cells at the fourth to seventh passage.

Preparation of Packaging Cells Expressing Retroviruses Encoding RhoA Mutants. RhoA variant cDNAs with previously established mutant functions were prepared by PCR amplification; the N19 and V14 mutations were engineered by incorporating the respective mutant codons in the coding regions of the sense-strand oligonucleotide primers, which also included nine bases of Kozak sequence ahead of the start codon. Clones were verified by sequencing. For fluorescent monitoring of retroviral transduction efficiency, a retroviral vector was designed for coexpression of GFP and Rho as separate proteins. This vector was engineered by subcloning unidirectionally the 1,360-bp *Xho*I/*Not*I restriction fragment from pIRES2-EGFP (Clontech catalog no. 6029-1) into the multicloning site of the retroviral vector pLCNX2 (Clontech catalog no. 6102-2). The fragment from pIRES2-EGFP includes multiple cloning sites, an internal ribosomal entry site, and the coding sequence for enhanced GFP. RhoA mutant cDNAs were inserted into the engineered vector (pLNCX2/IRES-EGFP), and properly oriented clones were identified by sequencing. PT67 retroviral packaging cells (Clontech), which express the 10A1 viral envelope for production of amphotropic virus, were transfected with pLNCX2/IRES-EGFP vector containing N19RhoA, V14RhoA, or vector without insert (control), and transfectants were cloned according to instructions. Clones expressing retrovirus at 1×10^5 colony-forming units (cfu)/ml were selected for subsequent experiments.

Retroviral Transduction of Dermal Microvascular ECs. Human dermal microvascular ECs at passage 5 or less were transduced with retroviruses according to a previously established, efficient method (16). VEGF (20 ng/ml) was added to enhance proliferation and survival during the transduction procedure that was

Abbreviations: VEGF, vascular endothelial growth factor; EC, endothelial cell.

*To whom correspondence should be addressed. E-mail: dsenger@caregroup.harvard.edu.

www.pnas.org/cgi/doi/10.1073/pnas.0308525100

repeated three times on consecutive days before subjecting cells to selection with 300 μg/ml G418. Selected populations were transduced 100% as indicated by GFP fluorescence, and cells were used within 1 week for experiments.

In Vitro* Assays with Transduced Microvascular ECs.** ***Measurement of Rho activity and staining of actin stress fibers. Active GTP-Rho (9×10^5 ECs per sample) was measure as described (17); blots were stained with rabbit polyclonal antibody to RhoA (Santa Cruz Biotechnology catalog no. SC-179). For F-actin staining, ECs on glass coverslips were fixed for 30 min in 3.7% buffered formaldehyde, washed with PBS, and stained with a solution of 1% BSA in PBS containing 0.1% Triton X-100 and Texas Red-labeled phalloidin (1:40 dilution; Molecular Probes) for 45 min. Next, coverslips were washed three times with PBS and mounted with Vectashield mounting medium (Vector Laboratories, Burlingame, CA). The Rho kinase inhibitor Y-27632 (in aqueous solution, catalog no. 688001) was purchased from Calbiochem. ***Cell organization and contractility in collagen gels.*** For assay of multicellular organization in three-dimensional collagen gels, ECs (1.6×10^5) were seeded in 12-well plates (Costar, Cambridge, MA) on a 1-ml cushion of 1 mg/ml neutralized rat tail collagen I (BD Bioscience, Bedford, MA) in medium, as described (18). At this density, ECs rapidly form a confluent monolayer. After 1 day, medium was removed and cells were overlaid with 1 ml of 1 mg/ml collagen I in medium identical to that used for the lower cushion. Cells were photographed 2 days later, by which time cells in the control and V14RhoA groups had reorganized into precapillary cords. Cord formation was quantified by morphometry, and a relative index of cord organization was calculated with the following formula: organizational index = 1.00 − (cord area/original monolayer area). Thus, as defined here, a larger numerical organizational index represents greater organization into cords. Cell number was measured as described for cell proliferation assays (see below). For collagen gel contraction assays, 250-μl cushions of 2 mg/ml collagen I were prepared in 48-well plates. Next, ECs (3×10^5 per well) were seeded in the same medium used for cord formation assays. After all cells had attached, medium was removed and cells were overlayed with fresh medium containing 250 μl of 2 mg/ml collagen I, which subsequently polymerized. Gel diameters were monitored with a dissecting microscope.

Proliferation and migration assays. Transduced ECs were seeded in collagen I-coated 48-well plates (Costar) at a density of 3,000 cells per well in medium consisting of EBM-2 (Clonetics, San Diego), 2% FBS, ± 20 ng/ml human recombinant $VEGF_{165}$. Cell number was determined on days indicated with the CyQuant Cell Proliferation assay (Molecular Probes). Chemotaxis and haptotaxis assays were performed as described (19). For the wound-scratch motility assay, cells were grown to confluence, and the monolayers were wounded identically with the narrow edge of a cell scraper (Falcon no. 35-3085, Becton Dickinson). Next, the medium was removed and replaced with EBM-2 containing 10% FBS and 10 ng/ml VEGF.

Angiogenesis Assay and Analyses of Blood Vessel Density, Blood Vessel Perfusion, and EC Organization *in Vivo*. Neovascularization was assayed *in vivo* according to an established method (19–21) with important modification to include retroviral packaging cells as a constant source of retrovirus. Seven-week-old female athymic nude mice were injected s.c. on right and left flanks with 0.5 cc of 9 mg/ml Matrigel (BD Bioscience) containing 1.5×10^6 SK-MEL2 human melanoma cells transfected for stable expression of human $VEGF_{165}$ together with 1.5×10^6 retroviral packaging cells, as indicated. Untransfected parental SK-MEL2 cells do not provoke angiogenesis detectably, and therefore the VEGF-SK-MEL2 transfectants used here allow for specific investigation of VEGF-driven angiogenesis (21). After 6 days, the animals in all groups were euthanized, dissected, and photographed. In addition, to analyze perfusion of new blood vessels, representative animals from each group received tail vein injections of 0.2 cc of 0.5% (wt/vol) Evan's Blue dye in sterile saline. Upon harvest, implants together with associated skin were fixed for 2 h in 10% buffered formalin and embedded in paraffin. Immunohistochemical staining of ECs with CD31 antibody, quantification of angiogenesis, and statistical analyses were performed as described (19). Retroviral transduction *in vivo* was confirmed by staining with antibody to GFP (Abcam, Cambridge, MA).

Results and Discussion

To investigate Rho function during neovascularization, we designed a highly versatile model of mouse skin angiogenesis that used VEGF-transfectants for continuous delivery of VEGF and retroviral packaging cells for continuous delivery of retrovirus. Angiogenic cytokine is required to drive angiogenesis, and we chose VEGF because it is centrally important for both normal and pathological angiogenesis (6–8). Retroviral packaging cells were engineered for expression of previously established dominant negative (N19) and active (V14) mutants of RhoA (22), and retrovirus lacking the RhoA insert served as control. As observed grossly at day 6 (Fig. 1), neovascularization was evident in the VEGF and VEGF plus V14RhoA groups as indicated by the presence of small tortuous, corkscrew-like blood vessels sprouting from larger preexisting vessels. However, retrovirus encoding dominant negative N19RhoA markedly inhibited neovascularization. Quantification of gross images indicated that N19RhoA inhibited the appearance of new blood vessels by 83% (±4% SE, $P < 0.001$). In contrast, coexpression of V14RhoA retrovirus together with VEGF markedly increased neovascularization by 116% (±5% SE, $P < 0.001$). The abundant newly formed small blood vessels in the V14RhoA group were rapidly perfused after tail vein injection of tracer (<10 min), and the rate of perfusion was indistinguishable from that of preexisting vessels (Fig. 1). Thus, these new blood vessels were functional and well integrated with the existing vascular network. When transfectants expressing VEGF were omitted from the Matrigel implants, angiogenesis did not occur, and the various retroviral packaging cell preparations alone did not stimulate angiogenesis (not shown). Thus, these experiments indicate that RhoA critically regulates angiogenesis driven by VEGF and that constitutively active RhoA can complement VEGF to increase angiogenesis by >100%, whereas dominant negative RhoA markedly inhibits VEGF-driven neovascularization. Parallel *in vitro* experiments, involving coculture of retroviral packaging cells and VEGF transfectants in the same proportions used *in vivo*, established that infection of VEGF-transfectants with either of the retroviruses did not alter VEGF expression as determined by quantitative immunoblotting of culture media (data not shown).

Immunohistochemical analyses of skin from the angiogenesis assays depicted grossly in Fig. 1 confirmed marked differences among the experimental groups. Mature blood vessels with lumens were rare in the VEGF plus N19RhoA group in comparison with the VEGF plus control retrovirus group, and blood vessels with lumens were particularly abundant in the VEGF plus V14RhoA group (Fig. 2*A*). Quantification of blood vessels with lumens in cross section indicated that these differences were highly significant (Fig. 2*B Right*). In contrast, quantification of EC density failed to detect significant differences among the VEGF, VEGF plus N19RhoA, and VEGF plus V14RhoA groups (Fig. 2*B Left*), indicating that the observed differences in blood vessel density reflected differences in EC organization rather than differences in EC number. Also, our findings that EC density in the VEGF, VEGF plus N19RhoA, and VEGF plus V14RhoA groups were indistinguishable from each other but high in comparison with the negative controls (i.e., no VEGF),

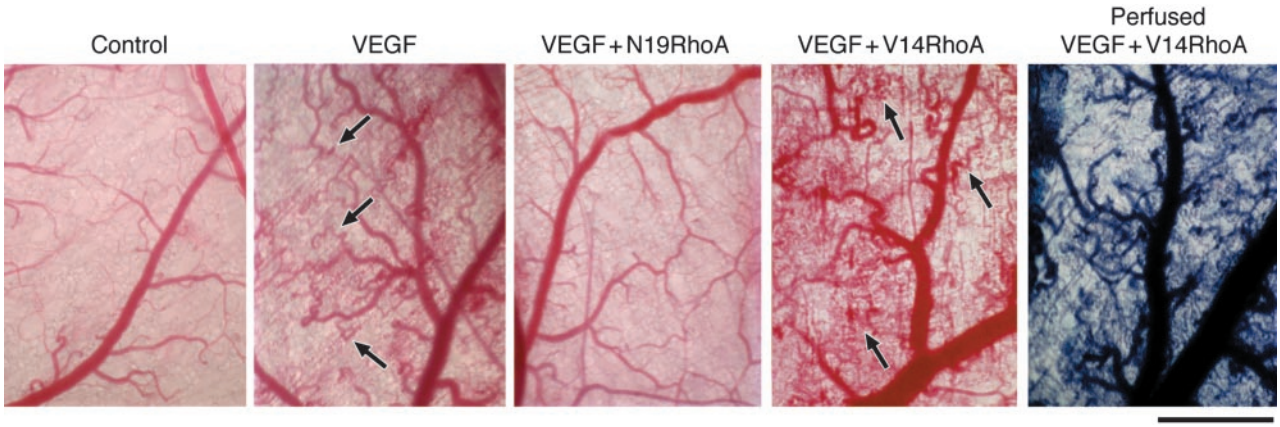

Fig. 1. RhoA mutants differentially regulate VEGF-driven angiogenesis in mouse skin. Retroviral packaging cells together with VEGF-transfectants (VEGF/SK-MEL2) were combined with basement membrane Matrigel and injected s.c. On day 6, animals were harvested and skin overlying the Matrigel implants was dissected. Control, negative control, i.e., Matrigel without cells; +VEGF, positive control consisting of VEGF transfectants plus packaging cells expressing retrovirus without Rho insert; VEGF + N19RhoA, VEGF transfectants plus packaging cells expressing retrovirus encoding dominant negative RhoA; VEGF + V14RhoA, VEGF transfectants plus packaging cells expressing retrovirus encoding an active RhoA mutant. Neither packaging cells nor untransfected SK-MEL2 cells provoked angiogenesis detectably (data not shown); therefore, angiogenesis depicted here is VEGF-dependent. V14RhoA cooperated with VEGF to promote the appearance of new blood vessels (characterized by tortuous, ''corkscrew'' appearance and marked with arrows) but N19RhoA was inhibitory. Moreover, abundant newly formed small blood vessels in the V14RhoA group were rapidly perfused (<10 min) after tail-vein injection of Evans blue dye tracer (*Far Right*). Photographs are representative examples of results consistently obtained in three separate experiments each with at least eight specimens per group. (Scale bar = 1 mm.)

are consistent with *in vitro* coculture experiments (above) indicating that VEGF expression was not affected by the presence of retrovirus encoding RhoA mutants. Because increased EC density is strictly dependent on VEGF expression in this model system (Fig. 2*B Left*), any significant differences in VEGF expression caused by retroviral transduction would have resulted in differences in EC density. However, no such differences were observed.

To define further the specific mechanisms through which the N19RhoA and V14RhoA mutants exert opposing effects on VEGF-stimulated neovascularization, human dermal microvascular ECs were transduced *in vitro* with retroviruses isolated from the packaging cells used in the animal experiments above. N19RhoA exhibits a mobility shift relative to endogenous Rho on SDS polyacrylamide gels; therefore, with immunoblotting, we were able to determine that expression of N19RhoA was expressed at ≈35% of endogenous Rho. Similarly, transduction with V14RhoA increased total Rho expression ≈35% above that observed in cells transduced with control retrovirus lacking insert. Consistent with this level of mutant RhoA expression, transduction with dominant negative N19RhoA, which is thought to act as a competitive inhibitor (23, 24), consistently suppressed total Rho activity by ≈20% as determined by Rhotekin-binding assays in multiple experiments (data not shown). In contrast, transduction with the active (GTP hydrolysis-defective) V14RhoA mutant consistently resulted a corresponding increase in Rho activity as indicated by Rhotekin-binding assays. Strikingly, and in agreement with the previously established importance of Rho for actin stress fibers (25) and cell contractility (26), transduction of dermal microvascular ECs with dominant negative N19RhoA reduced actin stress fibers (Fig. 3*A*) and prevented EC contraction of collagen I gels (Fig. 3*B*). Also, active V14RhoA induced actin stress fibers (Fig. 3*A*) and increased contraction of collagen I gels significantly (Fig. 3*B*). The Rho kinase inhibitor Y-27632 (27) acted similarly to N19RhoA in both assays (Fig. 3). Rho kinase (p160ROCK) is an immediate effector of RhoA (28), and we chose a 1 μM concentration of Y-27632 because the IC_{50} of this inhibitor for Rho kinase is ≈800 nM and because the available evidence indicates that 1 μM Y-27632 provides highly specific inhibition of Rho kinase (29). However, at higher concentrations (e.g., 10 μM), Y-27632 also inhibits other kinases (29). Because 1 μM Y-27632 was effective at reducing actin stress fibers and preventing contraction of collagen I gels similarly to N19RhoA, it is likely that N19RhoA mediates its inhibitory effects on EC stress fibers and contractility through suppression of Rho kinase activity. Finally, it is clear from the experiments presented in Fig. 3 that the levels of expression of these Rho mutants achieved in dermal microvascular ECs through retroviral transduction was sufficient to exert marked effects both on the assembly of actin stress fibers and on cell contraction of three-dimensional collagen I. These findings, together with our observations that total Rho activity, as measured with the Rhotekin-binding assay (17), was modestly affected by transduction with Rho mutants (≈20%), suggest that relatively small changes in Rho activity can strongly affect the contractility of microvascular ECs. Such observations are not without precedent. Even more modest expression of Rho kinase mutants (≈10% of endogenous wild-type Rho kinase) was found to markedly influence stress fiber formation and invasive behavior of hepatoma cells (30). Finally, consistent with our experiments implicating Rho and Rho kinase critically in EC contraction of collagen I gels (Fig. 3*B*), others have reported that both N19RhoA and Y-27632 (5 μM) suppressed EC contraction of three-dimensional Matrigel (31).

Next, we investigated the effects of these RhoA mutants for EC organizational behavior in collagen I gels. During angiogenesis, proliferating ECs organize to form new three-dimensional capillary networks through a process involving transition of endothelial precursor cells to a spindle-shape morphology (32) in combination with alignment into solid, multicellular, precapillary, cord-like structures (33). Moreover, these cord-like structures are interconnected to form a polygonal network (32, 34). Three-dimensional type I collagen provokes ECs in culture to undergo marked shape changes that closely imitate precapillary cord formation *in vivo* (34–36); consequently, embedding of ECs in collagen I is a useful strategy for investigating vascular morphogenesis. As shown in Fig. 4, transduction with V14RhoA promoted EC organization into cords, relative to controls; in contrast, both N19Rho and the Rho kinase inhibitor Y-27632 suppressed cord formation (Fig. 4*A*). Quantification of organi-

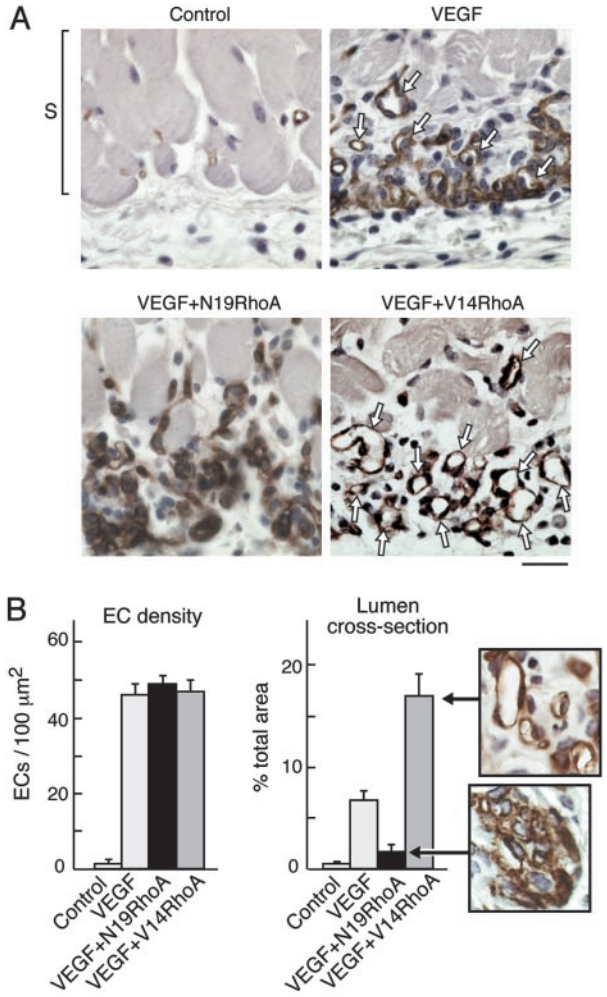

Fig. 2. RhoA mutants differentially regulate assembly of ECs into new blood vessels *in vivo*. (*A*) Skin specimens (day 6, as in Fig. 1) were fixed and embedded in paraffin, and ECs were stained for CD31. Staining of new ECs (brown), immediately below the smooth muscle cell layer (S), and at the interface between the host and the angiogenic stimulus, was strong in all experimental groups except the negative controls. New ECs of the VEGF group were only partially integrated into blood vessels with lumens (arrows). In contrast, new ECs of the V14RhoA plus VEGF group were highly integrated into new blood vessels with lumens (arrows), whereas new blood vessels with lumens were rare in the N19 RhoA plus VEGF group. Photographs are representative examples of results consistently obtained in two separate experiments; $n > 12$ for each group; bar = 25 μm. (*B*) Magnified views illustrate strong organization of ECs into blood vessels with lumens in the VEGF plus V14RhoA group and, in contrast, the failure of ECs in VEGF plus N19RhoA group to organize detectably. Such images were used for morphometric quantification of vascular cross-sectional area attributable to blood vessels with functional lumens (*Right*) and morphometric quantification of EC density (*Left*). Error bars = standard errors; $n > 20$ for each group. We observed no significant differences in EC density between the N19RhoA and V14RhoA groups; however, differences in cross-sectional area of blood vessel lumens were highly significant ($P < 0.001$).

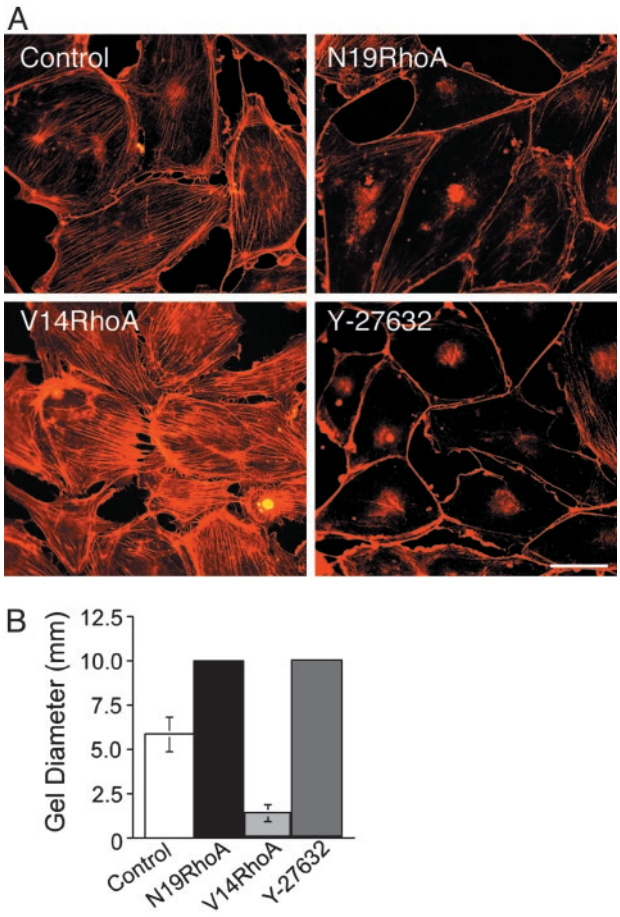

Fig. 3. RhoA mutants regulate microvasular EC actin stress fibers and contraction of collagen I gels *in vitro*. Human dermal microvascular ECs were transduced with retrovirus encoding active V14RhoA, dominant-negative N19RhoA, and retrovirus without insert (control). (*A*) Texas red-staining of actin stress fibers; Y-27632, Rho kinase inhibitor (1 micromolar final concentration, added 24 h prior). (Bar = 50 μm.) (*B*) Control transductants contracted collagen I gels, but N19RhoA and Y-27632 (1 μM, added at time 0) completely prevented contraction (10 mm = original gel diameter). In contrast, V14RhoA promoted significantly greater contraction of the gels relative to controls (error bars = standard deviations; $P < 0.001$).

zation by morphometry indicated that differences were highly significant and that differences were not attributable to inequalities in cell number (Fig. 4*B*). Thus, these *in vitro* experiments identify Rho activity as a critical regulator of retraction-mediated assembly of ECs into precapillary cords within a three-dimensional collagen matrix, and they directly link Rho activity to a morphogenetic process that imitates key aspects of EC organization during angiogenesis *in vivo*. In addition, they suggest that Rho kinase is a key effector through which Rho regulates cord formation.

In contrast to the stringent regulation by Rho observed for cord formation within three-dimensional collagen gels, we found no evidence that expression of either N19RhoA or V14RhoA or treatment with 1 μM Y-27632 affected microvascular EC proliferation (Fig. 5*A*). This finding is consistent with the histological analyses of angiogenesis *in vivo* (Fig. 2), indicating that EC density was not affected by N19RhoA or V14RhoA. In addition, we found no evidence that ECs transduced with N19RhoA or V14RhoA mutants or ECs treated with 1 μM Y-27632 exhibited differences in motility as determined in chemotaxis and haptotaxis assays (Fig. 5*B*) and in the wound-scratch motility assay (Fig. 5*C*). These findings are consistent with a previous report indicating that transduction of ECs with a Tat-N19Rho fusion protein did not alter migration, but they are not consistent with findings reported in the same manuscript indicating that Tat-V14Rho inhibited migration (37). However, the Tat–Rho fusion proteins appear to have resulted in greater intracellular concentrations of the Rho mutants relative to those achieved with retrovirus in our experiments, and this may explain the different consequences for EC migration. Also, others have reported that the Rho kinase inhibitor Y-27632 inhibited EC migration (38), but the dose used was 10 times the dose used in our experiments.

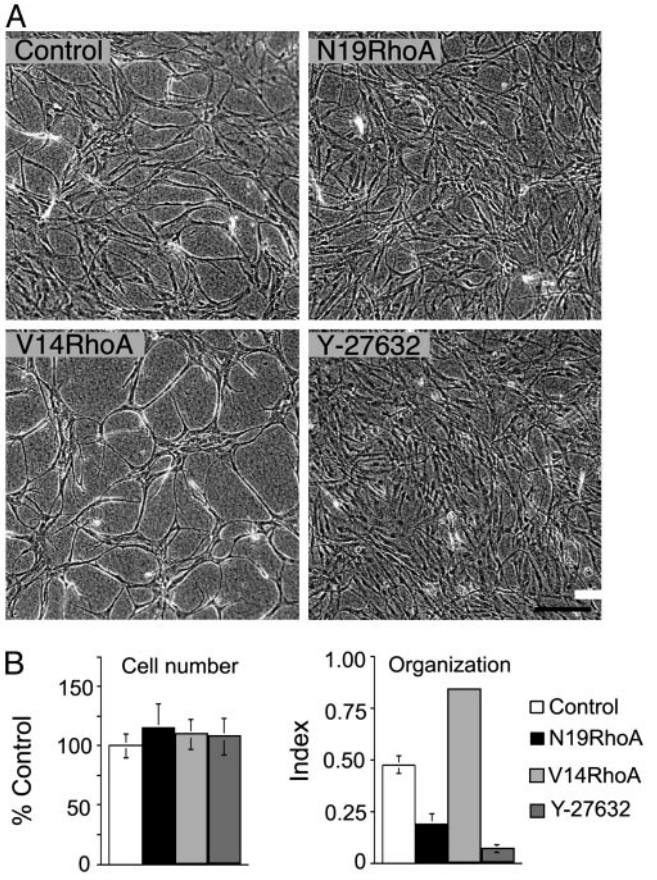

Fig. 4. RhoA mutants regulate EC organization into precapillary cords. (*A*) Confluent EC monolayers, consisting of equal numbers of cells, were established on collagen I gels and, 24 h later, were overlaid with collagen I. Note that, relative to controls, dominant negative N19RhoA inhibited retraction and reorganization of confluent ECs into precapillary cords and that active V14RhoA promoted cord formation relative to controls. Similar to N19RhoA, the Rho kinase inhibitor (1 μM Y-27632, added at time 0) inhibited cord formation. (Bar = 200 μm). (*B*) Cell numbers were indistinguishable in the different experimental groups, but quantification of EC assembly into cords with morphometry indicated that organizational differences (see *Materials and Methods*) were highly significant ($P < 0.001$, error bars = standard deviations).

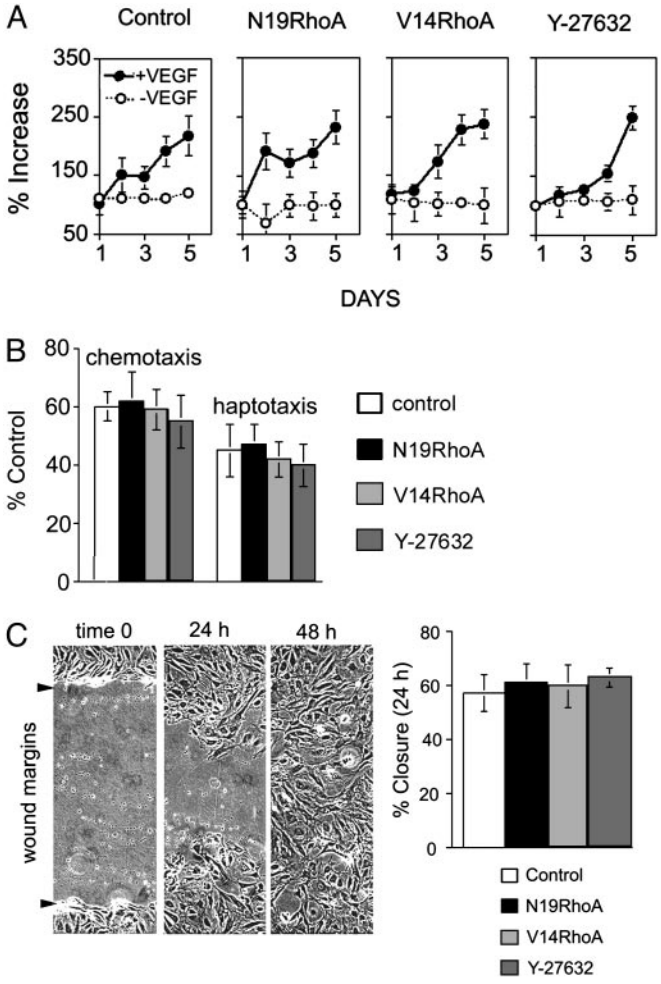

Fig. 5. Transduction with RhoA mutants did not regulate EC proliferation or migration detectably. (*A*) Proliferation assays performed in the presence (20 ng/ml) and absence of VEGF. (*B*) Chemotaxis assays (directed migration toward 20 ng/ml VEGF) and haptotaxis assays (directed cell migration toward collagen I). (*C*) For the wound-scratch motility assay, monolayers were wounded at time 0; each experimental cell population had closed the wound by 48 h (photographs are representative of all groups; arrows indicate original wound margins). Percent wound closure was determined at 24 h and was indistinguishable among the different groups. All experiments were repeated at least twice with similar results (error bars = standard deviations). Y-27632, Rho kinase inhibitor (1 μM, added at time 0 for all experiments).

In addition, others have reported that transduction with N19RhoA suppressed EC motility (31), but it appears that they achieved considerably greater inhibition of Rho activity (≈75%) in comparison with that achieved in our experiments (≈20%). Thus, the consequences of modulating Rho activity for EC migration may depend critically on percent change in Rho activity.

To summarize, the *in vitro* experiments presented in Figs. 3–5 define a selective function for Rho in regulating EC contractility and organization within three-dimensional collagen I; and these findings are entirely consistent with immunohistochemical analyses of the *in vivo* angiogenesis experiments (Fig. 2), which identified a selective function for Rho in regulating EC organization into new blood vessels. More specifically, both our *in vitro* and *in vivo* experiments support the conclusion that expression of dominant negative N19RhoA markedly inhibits VEGF-driven angiogenesis by interfering with EC organization into new blood vessels and, conversely, that the organization of ECs into new blood vessels during VEGF-driven angiogenesis can be substantially improved by expression of the active V14RhoA mutant. Consistent with these conclusions, sphingosine-1-phosphate has been shown to potentiate angiogenesis *in vivo*, and stimulation of vascular morphogenesis by this lipid *in vitro* is partially dependent on Rho, although it is also partially dependent on the GTPase Rac (39). Consistent with our *in vitro* data suggesting that the inhibitory action of N19RhoA toward EC organization in collagen I is mediated by Rho kinase, the Rho kinase inhibitor Y-27632 was found to inhibit angiogenesis in the developing chick chorioallantoic membrane (40), although Rho function in neovascularization was undefined. Interestingly, the GTPases Rac and Cdc42 have been implicated in the formation of vacuoles and lumens, and Rac has been implicated in regulating EC shape during capillary morphogenesis *in vitro* (41, 42). Therefore, it is likely that other GTPases in addition to Rho control angiogenesis *in vivo*; however, based on current understanding of the functions of Rho, Rac, and Cdc42 in other systems (9, 10), the mechanistic contributions of each will likely prove to be different.

Finally, therapies designed to suppress angiogenesis offer considerable promise for controlling important pathologies such

as proliferative retinopathies (43, 44) and cancer (4, 44). Conversely, for treatment of disorders involving critical vascular insufficiency, including chronic skin lesions, there is strong motivation to identify therapies for enhancing neovascularization (5, 44). Depending on whether the clinical goal is to inhibit or stimulate angiogenesis, emphasis thus far has focused largely on strategies designed either to suppress or stimulate EC proliferation and survival. Studies described here define a distinctly different but complementary approach. Specifically, our experiments demonstrate that manipulation of Rho activity can be used either to suppress or enhance the organizational behavior of ECs and thereby markedly suppress or enhance the formation of new blood vessels. Collectively, these studies illustrate the practical importance of regulating vascular morphogenesis in combination with EC proliferation, and they provide the foundation for design of new rational strategies to control neovascularization.

We thank Martin Schwartz for generously providing the GST-Rho-binding domain construct, and Lois Smith and Arthur Mercurio for helpful discussions. This work was supported by U.S. Public Health Service Grant CA77357 from the National Cancer Institute and by the V. Kann Rasmussen Foundation.

1. Folkman, J. & Shing, Y. (1992) *J. Biol. Chem.* **267,** 10931–10934.
2. Rafii, S. (2000) *J. Clin. Invest.* **105,** 17–19.
3. Aiello, L. P., Pierce, E. A., Foley, E. D., Takagi, H., Chen, H., Riddle, L., Ferrara, N., King, G. L. & Smith, L. E. H. (1995) *Proc. Natl. Acad. Sci. USA* **92,** 10457–10461.
4. Folkman, J. (1995) *N. Engl. J. Med.* **333,** 1757–1763.
5. Isner, J. M. & Asahara, T. (1999) *J. Clin. Invest.* **103,** 1231–1236.
6. Dvorak, H. F., Brown, L. F., Detmar, M. & Dvorak, A. M. (1995) *Am. J. Pathol.* **146,** 1029–1039.
7. Ferrara, N. (2002) *Nat. Rev. Cancer* **2,** 795–803.
8. Pierce, E. A., Avery, R. L., Foley, E. D., Aiello, L. P. & Smith, L. E. H. (1995) *Proc. Natl. Acad. Sci. USA* **92,** 905–909.
9. Hall, A. (1998) *Science* **279,** 509–514.
10. Ridley, A. (2001) *Trends Cell Biol.* **11,** 471–477.
11. Barrett, K., Leptin, M. & Settleman, J. (1997) *Cell* **91,** 905–915.
12. Hacker, U. & Perrimon, N. (1998) *Genes Dev.* **12,** 274–284.
13. Brock, J., Midwinter, K., Lewis, J. & Martin, P. (1996) *J. Cell Biol.* **135,** 1097–1107.
14. Richard, L., Velasco, P. & Detmar, M. (1998) *Exp. Cell Res.* **240,** 1–6.
15. Senger, D. R., Ledbetter, S. R., Claffey, K. P., Papadopoulos-Sergiou, A., Peruzzi, C. A. & Detmar, M. (1996) *Am. J. Pathol.* **149,** 293–305.
16. Le Doux, J. M., Landazuri, N., Yarmush, M. & Morgan, J. R. (2001) *Hum. Gene Ther.* **12,** 1611–1621.
17. Ren, X. D., Kiosses, W. B. & Schwartz, M. A. (1999) *EMBO J.* **18,** 578–585.
18. Ilan, N., Mahooti, S. & Madri, J. A. (1998) *J. Cell Sci.* **111,** 3621–3631.
19. Senger, D. R., Perruzzi, C. A., Streit, M., Koteliansky, V. E., de Fougerolles, A. R. & Detmar, M. (2002) *Am. J. Pathol.* **160,** 195–204.
20. Passaniti, A., Taylor, R. M., Pili, R., Guo, Y., Long, P. V., Haney, J. A., Pauly, R. R., Grant, D. S. & Martin, G. R. (1992) *Lab. Invest.* **67,** 519–528.
21. Senger, D. R., Claffey, K. P., Benes, J. E., Perruzzi, C. A., Sergiou, A. P. & Detmar, M. (1997) *Proc. Natl. Acad. Sci. USA* **94,** 13612–13617.
22. Qui, R.-G., Chen, J., McCormick, F. & Symons, M. (1995) *Proc. Natl. Acad. Sci. USA* **92,** 11781–11785.
23. Feig, L. A. (1999) *Nat. Cell Biol.* **1,** E25–E27.
24. Symons, M. & Settleman, J. (2000) *Trends Cell Biol.* **10,** 415–419.
25. Ridley, A. J. & Hall, A. (1992) *Cell* **70,** 389–399.
26. Burridge, K. & Chrzanowska-Wodnicka, M. (1996) *Annu. Rev. Cell Dev. Biol.* **12,** 463–518.
27. Ishizaki, T., Uehata, M., Tamechika, I., Keel, J., Nonomura, K., Maekawa, M. & Narumiya, S. (2000) *Mol. Pharmacol.* **57,** 976–983.
28. Ishizaki, T., Naito, M., Fujisawa, K., Maekawa, M., Watanabe, N., Saito, Y. & Narumiya, S. (1997) *FEBS Lett.* **404,** 118–124.
29. Davies, S. P., Reddy, H., Caivano, M. & Cohen, P. (2000) *Biochem. J.* **351,** 95–105.
30. Itoh, K., Yoshioka, K., Akedo, H., Uehata, M., Ishizaki, T. & Narumiya, S. (1999) *Nat. Med.* **5,** 221–225.
31. Cascone, I., Giraudo, E., Caccavari, F., Napione, L., Bertotti, E., Collard, J. G., Serini, G. & Bussolino, F. (2003) *J. Biol. Chem.* **278,** 50702–50713.
32. Drake, C. J. & Little, C. D. (1999) *J. Histochem. Cytochem.* **47,** 1351–1355.
33. Drake, C. J., Brandt, S. J., Trusk, T. C. & Little, C. D. (1997) *Dev. Biol.* **192,** 17–30.
34. Vernon, R. B., Lara, S. L., Drake, C. J., Iruela-Arispe, M. L., Angello, J. C., Little, C. D., Wight, T. N. & Sage, E. H. (1995) *In Vitro Cell. Dev. Biol.* **31,** 120–131.
35. Delvos, U., Gajdusek, C., Sage, H., Harker, L. A. & Schwartz, S. M. (1982) *Lab. Invest.* **46,** 61–72.
36. Montesano, R., Orci, L. & Vassalli, P. (1983) *J. Cell Biol.* **97,** 1648–1652.
37. Soga, N., Namba, N., McAllister, S., Cornelius, L., Teitelbaum, S. L., Dowdy, S. F., Kawamura, J. & Hruska, K. (2001) *Exp. Cell Res.* **269,** 73–87.
38. van Nieuw Amerongen, G. P., Koolwijk, P., Versteilen, A. & van Hinsbergh, V. W. M. (2003) *Arterioscler. Thromb. Vasc. Biol.* **23,** 211–217.
39. Lee, M. J., Thangada, S., Claffey, K. P., Ancellin, N., Liu, C. H., Kluk, M., Volpi, M., Sha'afi, R. I. & Hla, T. (1999) *Cell* **99,** 301–312.
40. Uchida, S., Watanabe, G., Shimada, Y., Maeda, M., Kawabe, A., Mori, A., Arii, S., Uehata, M., Kishimoto, T., Oikawa, T. & Imamura, M. (2000) *Biochem. Biophys. Res. Commun.* **269,** 633–640.
41. Bayless, K. J. & Davis, G. E. (2002) *J. Cell Sci.* **115,** 1123–1136.
42. Connolly, J. O., Simpson, N., Hewlett, L. & Hall, A. (2002) *Mol. Biol. Cell* **13,** 2474–2485.
43. Smith, L. E., Shen, W., Perruzzi, C., Soker, S., Kinose, F., Xu, X., Robinson, G., Driver, S., Bischoff, J., Zhang, B., *et al.* (1999) *Nat. Med.* **5,** 1390–1395.
44. Ferrara, N. & Alitalo, K. (1999) *Nat. Med.* **5,** 1359–1364.